Indian Journal of Pure & Applied Physics
Vol. 64, July 2026, pp. 730-736
DOI: 10.56042/ijpap.v64i7.29251

Bias-Field-Dependent Impedance and Phase Characterization of a Ferroelectric Liquid Crystals Relevant to Display Applications

Surjya Sarathi Bhattacharyya[a*] & Amrita Mukherjee[b]

[a]Department of Physics, Asutosh College, 92, Shyamaprasad Mukherjee Road, Kolkata, 700 026, India

[b]Department of Physics, Jogamaya Devi College, 92, Shyamaprasad Mukherjee Road, Kolkata, 700 026, India

Received: 1st March 2026; accepted: 3rd June 2026

Phase transition and dielectric relaxation dynamics of a ferroelectric liquid crystal (FLC) material were investigated across the SmC*–N* phase transition using differential scanning calorimetry (DSC) and impedance spectroscopy under applied DC bias fields. Dielectric spectra recorded under DC bias exhibit anomalous low-frequency behavior in the vicinity of the SmC*–N* transition. A pronounced enhancement of low-frequency dielectric absorption is observed at low DC bias fields, followed by suppression at higher bias fields near ~72 °C, accompanied by the presence of the conventional Goldstone mode at slightly higher frequencies. The dielectric response over a wide temperature range, analyzed using a Cole–Cole–modified Debye model in both biased and unbiased conditions, reveals significant variations in the relaxation parameters. The low-frequency relaxation process close to the SmC*–N* transition is attributed to the combined contributions of the Goldstone mode and domain-related dynamics, as evidenced by the anomalous DC bias dependence of the dielectric parameters. The temperature dependance of relaxation parameters under DC bias exhibits conventional Goldstone-mode-like behavior due to suppressed domains and field-induced alignment of the spontaneous polarization.

Keywords: Ferroelectric liquid crystals, Phase transition, Dielectric relaxation, Polarization

1 Introduction

Ferroelectric Liquid crystal (FLC) systems have instigated researchers in recent times for their application potential in display devices. The invention of bi-stability and sub-millisecond response time of ferroelectric liquid crystal in surface stabilized geometry by N.A. Clark and S.T Lagerwall[1] started the trend. But, significantly higher driving voltage, limited gray scale ability, alignment defect and image sticking issues have limited their commercial viability. In order to improve gray scale ability diverse research teams has put forward different LC driving modes. To name a few viz. twisted smectic[2], active-matrix FLC[3], vertical aligned display using deformed helix FLC[4], V-Shaped switching[5] etc. Among them V-Shaped switching display mode in FLCs offers several distinct advantages in terms of response speed, simpler electronic driving circuitry and higher contrast ratio made it an important development in the history of flat-panel display technology[6]. However, since pixels respond equivalently in the V-shaped switching mode to both positive and negative voltage cycles above the threshold, non-selected rows receiving partial voltages can trigger unintended switching. This leads to image degradation, flickering, and cross-talk, thereby causing problems in passive matrix displays. Hence half-V switching mode was discovered in FLC displays where selective addressing, grayscale control and cross-talk suppression plays crucial role. Moreover, high spontaneous polarization (P_S) > 50nC/cm^2 and moderate pitch length ~ 1 µm of host FLC material played crucial role in development of V-shaped switching liquid crystal devices[5,7]. Alternatively, for half-V switching mode requires lower or asymmetrically tuned P_S which reduces switching under reverse polarity while investigated in asymmetrical hybrid cell[8]. Thus, FLC materials having low P_S along with Half-V mode LC driving scheme was proposed. In such material designs, the occurrence of the Smectic A phase is generally suppressed,[3,9] resulting in a direct transition from the ferroelectric SmC* phase to the N* phase. This intrinsic property enables continuous grayscale modulation, making these materials well-suited for active matrix display applications. However, while cooling from N* to SmC* phase both up and down domains persists, leading to horizontal chevron alignment defect.

*Corresponding author:
E-mail: surjyasarathi.bhattacharyya@asutoshcollege.in

Characterizing the precise evolution of these domain configurations and evaluating the electrical impact of such alignment defects requires a highly sensitive probe. In this regard impedance spectroscopy has played a very important role in understanding molecular dynamics and map relaxation modes of polar liquid crystal systems providing precise information on the relaxation mechanisms of both collective and non-collective forms under various mesophases. Recently, the use of impedance spectroscopy has been indispensable in the analysis of phase behavior in the newly discovered ferroelectric nematic (N_F) phases with regards to their dual collective relaxation mechanism[10], distinct phason modes[11], separation of bulk contributions from electrode polarization phenomena[12], and hyper-dielectric effects in multifunctional ferronematics[13]. Moreover, the application of impedance spectroscopy combined with DC bias measurements can provide insights into structural symmetry breaking of enantiomeric versus racemic smectic mixtures by revealing high-frequency librations such as the bias-independent X-mode when macroscopic polarization is eliminated[14].

While materials showing SmC* phase has also been studied exhaustively using impedance spectroscopic method in last few decades, investigations targeting samples undergoing direct SmC* to N* phase is limited[15, 16, 17] primarily due to the challenges associated with sample alignment[18, 19]. The FLC material under investigation exhibits a direct SmC*–N* phase transition and is commercially used in Half-V switching mode for active matrix display devices. It features a broad ferroelectric phase range, moderate spontaneous polarization, and a notably short helical pitch[8, 20]. Despite their potential, a comprehensive phase characterization of these systems under varying bias field and temperatures-specifically via impedance spectroscopy remains largely unexplored. Consequently, this paper details a rigorous analysis of the dielectric relaxation dynamics within a FLC commonly utilized in Half-V switching mode.

2 Experimental Details

The sample under investigation viz. Felix R3206 [8, 20] possessing the sequence of phases: Iso. – 109.9 ^{0}C – N* – 79.6^{0}C-- SmC* - -17.9^{0}C Cr has been investigated. The room temperature physical properties of Felix R3206 in ambient conditions are spontaneous polarization (P_S) =20.1 nC/cm^2, pitch = 0.8 ±0.2 μm. The FLC samples were introduced into custom-fabricated cells (thickness ≈ 12 μm; active area ≈ 16 mm^2) via capillary action in isotropic phase similar to previous reports[21,22]. Cells were fabricated using transparent conducting indium tin oxide (ITO) coated glasses. To prepare the substrates, a polyvinyl alcohol (PVA) alignment layer was spin-coated onto the glass plates and subsequently annealed at 140°C for 2hr. PVA strongly promotes planar alignment with a negligible or zero pretilt angle, which is essential to achieve homogeneous planar alignment of LC[23]. Substrates were unidirectionally rubbed and antiparallelly sandwiched with mica spacers maintaining uniform cell gap. Hence, they were calibrated using toluene and air as standard references. The sample temperature was regulated using Mettler FP82 hot stage conjugated to Mettler FP90 controller with an accuracy of ±0.1^{0}C. An HP-4192A impedance analyzer, integrated with a computer control system, was employed for all dielectric measurements.

3 Results and Discussion

3.1 Differential Scanning Calorimetric (DSC) Measurements

DSC thermograms are recorded in heating and cooling protocols for the samples are shown in Fig. 1. The sample is heated with a scan rate of 10 °C/min and thermally stabilized at isotropic temperature for 2 minutes followed by cooling run at same scan rate. DSC thermograms exhibit prominent endothermic and exothermic peaks during respective heating and cooling run around phase boundary of SmC*-N* and N*-Isotropic phases for the sample. The order – disorder type Nematic to Isotropic transition is

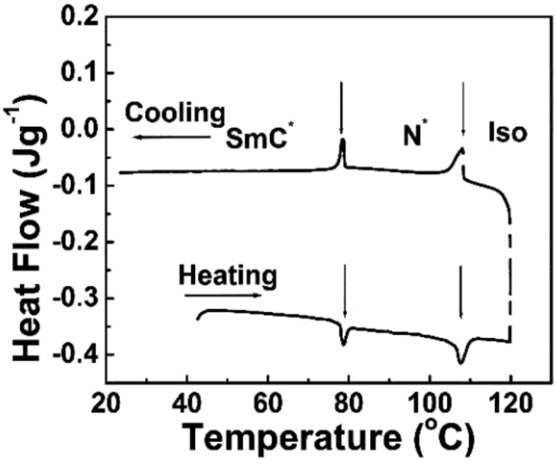

Fig. 1 — DSC thermogram of the sample under heating and cooling run showing SmC*-N* and N*-Isotropic Phase transitions

necessarily first order in nature as evident from DSC thermogram of FLC. DSC thermogram clearly exhibits higher change in enthalpy due to N*-Isotropic transition in comparison with SmC*-N*. The N*-Isotrpic transition temperature for the sample obtained as ~ 107.7 °C during heating and 108.1 °C during cooling and SmC*-N* phase transition temperature for ~78.7 °C during heating and ~78.5 °C during cooling. The material thus demonstrates a marginal hysteretic effect during thermal cycling. The SmC*-N* phase transition demonstrates the characteristics of a weakly first-order nature as DSC thermogram exhibit slight change in slope.

3.2 Dielectric Measurements

The nature of phase transitions was further examined using temperature (T) dependent dielectric permittivity (ε'). Figure 2 shows temperature dependent permittivity for the sample recorded at 70 kHz frequency. Sufficiently high frequency permittivity has been reported to avoid effect of ions and low frequency relaxation process. The SmC*-N* transition in FLC has been recorded as a small hump in the ε'-T plot whereas the N*-Isotropic transition shows a significantly higher peak. At the vicinity of SmC*-N* transition has been shown the $1/(\varepsilon')$-T plot in the inset. Interesting non-linear and shallow dip followed by flat region between 78 ^{O}C and 79 ^{O}C reenforces weak first order nature of SmC*-N* transition. The N*-Isotropic transition has been depicted by the peak in ε'-T plot at ~ 108 ^{O}C indicating first order nature of the transition.

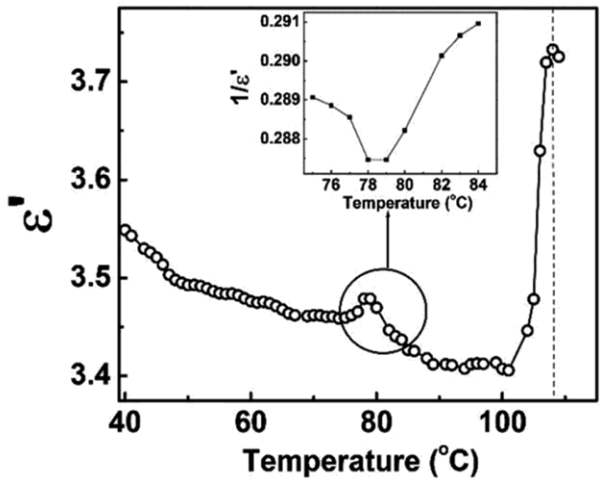

Fig. 2 — Real part of dielectric permittivity (ε′) at 70 kHz frequency, as a function of temperature exhibiting SmC*-N* and N*-Isotropic Phase transitions. Inset shows inverse of dielectric permittivity in the vicinity of SmC*-N* phase transition

The frequency dependent real and imaginary part of dielectric permittivity at different applied DC bias voltages are reported at 72 ^{O}C in SmC* phase is depicted in Fig. 3 (a) and (b) respectively. Measurements were conducted at 2-minute intervals to minimize any potential influence of one measurement on another. A prominent low frequency relaxation process is noticeable along with a second relaxation peak at slightly higher frequency in absence of applied external DC bias. The DC bias field dependent permittivity and absorption spectra show anomalous behavior. In presence of weak DC bias, (viz. up to 1.0 V) the dielectric absorption appears to enhance, however, slowly enhancing DC bias further shows suppression of the absorption peak. This is interesting to mention here that such anomalous DC bias field induced dielectric dispersion has been reported in the literature[24]. Although ionic motion can contribute to low-frequency dielectric losses under DC bias, several observations indicate that the enhanced absorption observed near the SmC*–N* phase boundary is predominantly governed by collective relaxation dynamics. The relaxation occurs at frequencies significantly higher than the characteristic ionic relaxation and shows a non-monotonic DC field dependence, inconsistent with simple ionic drift or electrode polarization. Furthermore, the suppression of dielectric absorption

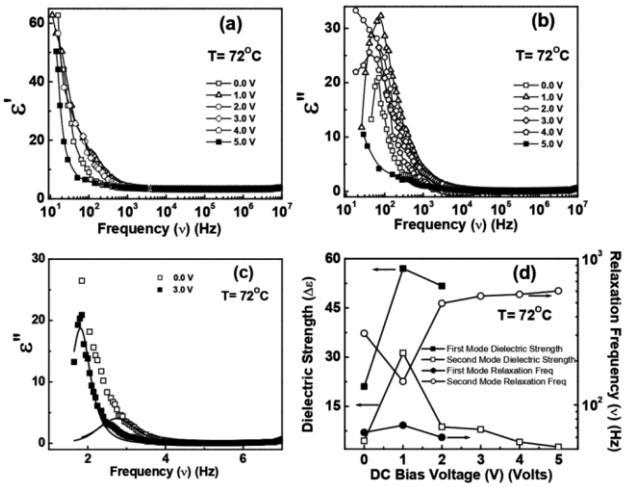

Fig. 3 — Real (ε′) (a) and Imaginary (ε′′) (b) part of dielectric permittivity as a function of frequency (ν) for different applied DC bias Voltages at 72 °C. (c) Imaginary (ε′′) part of dielectric permittivity represented as scattered points and the solid line corresponds to the Cole-Cole fitting at 72 °C in absence and 3.0V DC bias. (d) Dielectric strength (Δε) and Relaxation frequency (ν) as a function different applied DC Bias voltages are shown, for first and second relaxation modes at 72 °C

at higher bias fields correlates with field-induced domain alignment and Goldstone-mode stiffening, whereas ionic contributions are expected to increase monotonically with applied field.

The experimental complex dielectric permittivity data were analyzed using the Cole-Cole modified theory[25] of Debye. According to this model, the angular frequency ω (= 2πν, ν is linear frequency), dielectric strength $\Delta\varepsilon = \varepsilon_S - \varepsilon_\infty$ (ε_S is the static dielectric permittivity and ε_∞ is the high frequency dielectric constant) and relaxation time $\tau = 1/2\pi\nu$ obey the following dispersion equation viz.

$$\varepsilon^* - \varepsilon_\infty = \frac{\Delta\varepsilon}{1+(i\omega\tau)^{(1-\alpha)}} \quad \ldots (1)$$

In Eq. (1) ε^* denotes complex dielectric permittivity. The parameter α serves as a measure of the distribution of relaxation times, while α=0 corresponds to a monodispersed (Debye-type) relaxation, higher values indicate a broader distribution of relaxation times within the system. Figure 3 (c) depicts the dielectric absorption for DC biases of 0.0 V and 3.0 V, where the scattered points represent experimental data and the continuous lines represent the best fit to Eq. (1). The absence of first relaxation peak is noticeable at 3.0V DC bias. The DC Bias field induced variation of dielectric strength ($\Delta\varepsilon$) and relaxation frequency (υ) for both the modes are shown in Fig. 3 (d). The dielectric strength of first relaxation mode significantly increases upon application of 1.0V DC bias followed by noticeable reduction at 2.0V. The relaxation frequency of the first relaxation mode does not appear to show significant variation and the mode disappears in presence of higher DC bias fields. The dielectric strength of second relaxation mode exhibits an initial enhancement at 1.0V DC bias followed by a monotonic reduction at higher DC bias fields. Concurrently, the relaxation frequency shows a dip at 1.0V before demonstrating a monotonically increasing trend at elevated biases.

The anomalous DC bias field induced changes observed in the dielectric absorption spectra, alongside corresponding variations in dielectric strength and relaxation frequency suggest that the first relaxation mode is governed by a domain relaxation process. Half-V mode FLC materials cooled from N* to SmC* phase is well known for exhibiting horizontal chevron alignment defects with distinctly up and down pointed spontaneously polarized domains but non-uniquely aligned along the rubbing direction of liquid crystal cells while top and bottom substrates are symmetrically antiparallelly aligned, as in our case[8, 9]. The application of DC bias strongly influences both the sizes and macroscopic alignment of these domains. Under weak DC bias field viz. ~ 1.0 V in our case, the domains likely orient and align along field direction resulting in an enhanced dielectric absorption. Enhancing the DC bias field further, the domains collapses so as the reduction of dielectric strength of first relaxation peak in dielectric absorption from 1.0 V to 2.0 V DC bias and monodomains formation is confirmed by disappearance of low frequency peak at ~ 3.0 V DC bias and above. The identified distinct relatively higher frequency second relaxation peak is attributed to Goldstone mode. In FLC materials, this process originates from small-angle fluctuations of the director's azimuthal angle. The applied DC bias field pins this azimuthal angle along the field direction, forcing the inherent macroscopic helical structure to unwind. The unwinding mechanism perfectly explains the observed- field dependent trends. At a weak bias of 1.0 V, the initial helical distortion or stretching leads to a structural softening, causing the characteristic dip in relaxation frequency alongside a momentary enhancement in dielectric strength. As the bias is elevated further, the field-induced pinning hardens the system, shifting the relaxation frequency upward while monotonically suppressing the dielectric strength. Notably, because the dominant domain mode contribution in our system is significantly intense and lies in close proximity to Goldstone mode frequency, these distinct features become cleanly resolvable only at relatively higher DC biases of 2.0 V and above, where the neighboring domain structures have begun to collapse.

Figure 4 shows the semicircular $\varepsilon' - \varepsilon''$ plot at a few exemplary temperatures viz. 40 °C, 60 °C and 72 °C for the samples in absence of DC bias. The scattered points represent the experimentally recorded results whereas the continuous line exhibits the best fitted curves in accordance with Eq. (1). The determined magnitude of distribution parameter (α) slightly higher than 0.1, indicating poly-dispersive nature of the modes. As discussed earlier the low frequency relaxation behavior in FLC sample might be attributed to combined contribution of Goldstone

mode and domain mode. The temperature variation of best fitted dielectric parameters viz. dielectric strength (Δε) and relaxation frequency (ν) in absence of DC bias and in presence of 5.0 V DC bias field is depicted in Fig. 5 (a) and (b) respectively. It is interesting to mention here that, the temperature dependent variation of the parameters for the FLC sample under investigation undergoing a direct SmC*–N* phase transition shows characteristics that are not signatures of a homogeneous SmC* phase governed solely by the conventional Goldstone mode. In the non-existence of an external DC bias field, the dielectric strength shows increasing trend with increasing temperature, attains a maximum, and then gradually decreases, eventually disappearing above approximately 76 °C as shown in Fig. 5 (a). Simultaneously, the relaxation frequency moves toward lower values with rising temperature, and its magnitude decreases from few hundreds of heartz to sub-hundred hertz range. Such behavior deviates from the expectations of the standard Goldstone-mode description and indicates the presence of additional relaxation mechanisms near the phase boundary.

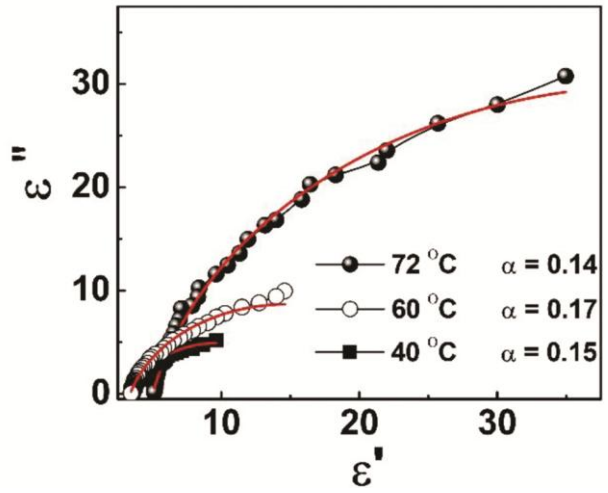

Fig. 4 — Real (ε′) vs Imaginary (ε′′) part of dielectric permittivity represented as scattered points and the solid line corresponds to the Cole-Cole fitting at 40°C, 60°C & 72 °C in absence of DC bias. The distribution parameters (α) are also depicted

In ferroelectric SmC* phases, the dominant low-frequency dielectric relaxation is generally attributed to the Goldstone mode, which commences from azimuthal fluctuations of the spontaneous polarization associated with the broken continuous rotational symmetry of the tilted phase[26–28]. Hence, the dielectric strength of the Goldstone mode is expected to increase monotonically as the SmC*–N* transition is approached from lower temperature due to the softening of the restoring torque, while the relaxation frequency typically increases with temperature due to anticipated decreasing trend of rotational viscosity with increasing temperature[27–29]. The observed non-monotonic dielectric strength and the anomalous decrease in relaxation frequency therefore suggest that the dielectric response near the transition cannot be designated to a single intrinsic mode.

A systematic explanation for such trends can be obtained recognizing the manifestation of SmC* domains in the vicinity of the SmC*–N* phase boundary. In direct SmC*–N* transitions, strong coupling between the tilt order parameter, spontaneous polarization, and chirality can give rise to spatially inhomogeneous states near the transition temperature[30–32]. As a consequence, the presence of finite-sized SmC* domains can be predicted within an

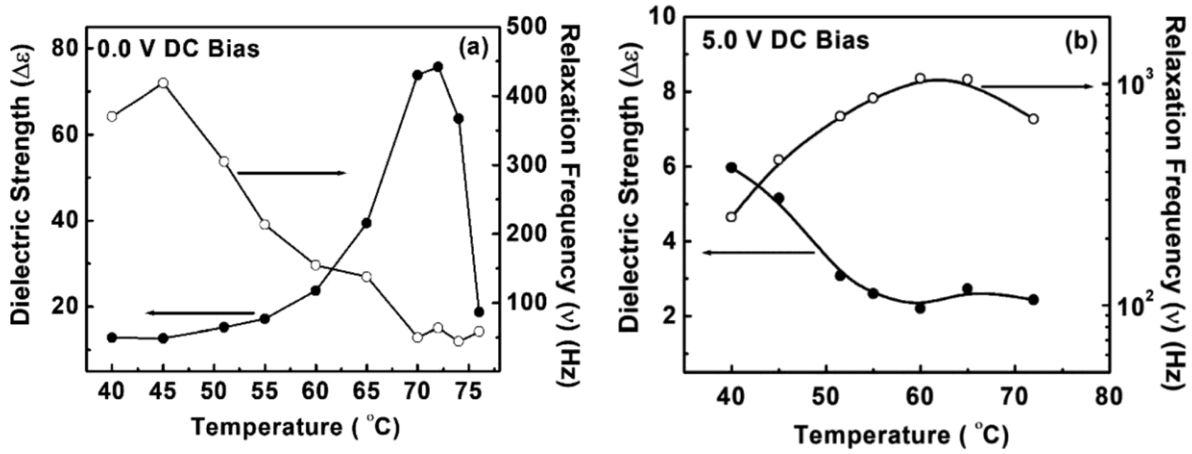

Fig. 5 — Dielectric strength ($\Delta\varepsilon$) and relaxation frequency (ν) as a function of temperature for (a) 0.0 V DC bias and (b) 5.0 V DC bias voltages are shown

emerging N* matrix over a finite temperature range. The low-frequency dielectric response increases significantly due to the additional polarization introduced by these domains. They exhibit interfacial dynamics, such as collective domain-wall motion, which further enhances the dielectric response in the low-frequency regime. In the SmC*–N* transition region, the dielectric strength increases and reaches a maximum. This behaviour may be attributed to enhanced polarizability arising from domain interactions near the phase transition. Thus, at transition temperature the permittivity of the SmC* domains and their interfaces attain its limit, as a consequence the dielectric strength also reaches its highest value. With the increase in temperature these domains begin to shrink and subsequently the spontaneous polarization decreases. So, the corresponding dielectric strength also decreases steadily until it eventually disappears in the N* phase. At the same time, the relaxation frequency was observed slows down. This might happen because of slower, domain-driven movements begin to take over from the faster Goldstone mode. It's also a sign of increased 'drag' or damping, caused by intense fluctuations and the messy boundaries between the SmC* and N* phases as they meet.

To support this mentioned interpretation, dielectric measurements has been performed under viz. 5.0 V DC bias field. When bias field was applied, the low-frequency dielectric strength is strongly reduced. It shows much weaker variation with temperature, while the relaxation frequency exhibits an increasing trend with temperature and assumes slightly higher values. The applied DC field aligns the spontaneous polarization, thereby suppressing domain formation and domain-wall motion. As a result, the contribution from domain-related relaxation processes is significantly reduced. Under mentioned conditions, the dielectric response is dominated primarily by the intrinsic Goldstone mode, whose dielectric strength is reduced due to field-induced stiffening of azimuthal fluctuations, while its relaxation frequency increases with temperature in accordance with conventional theoretical studies. Thus, the contrasting temperature dependence of dielectric parameters in the absence and presence of a DC bias field provides compelling evidence that the anomalous behaviour of dielectric strength and relaxation frequency near the SmC*–N* transition originates from the coexistence of conventional Goldstone mode relaxation and slower, domain-mediated processes within the phase-boundary region. Similar dielectric anomalies associated with the pre-transitional SmC* phase and weakly first-order transitions have been reported in several ferroelectric liquid-crystal systems, further supporting the present interpretation[31-33].

4 Conclusion

Differential scanning calorimetry (DSC) and static dielectric permittivity measurements confirm the SmC*–N* phase transition at ~78–79 °C, is weakly first order in nature, and also the N*–Isotropic transition at ~108 °C, which is first order. Anomalous behavior near the SmC*–N* transition region is revealed by dielectric spectroscopy. A pronounced enhancement of the low-frequency dielectric absorption is observed at low DC bias fields, followed by suppression at higher bias fields close to the SmC*–N* transition temperature (≈72 °C), along with the presence of the expected Goldstone mode at slightly higher frequencies. Analysis of the dielectric spectra over a wide temperature range using a Cole–Cole–modified Debye model, both in the presence and absence of DC bias has been done in detail which reveals significant variations in the obtained relaxation parameters. The low-frequency relaxation process observed in the vicinity of the SmC*–N* transition reflects contributions from the conventional Goldstone mode coupled with domain-related dynamics, as evidenced by the anomalous DC bias field dependence of the dielectric parameters. These anomalies are attributed to the coexistence of intrinsic Goldstone-mode relaxation and slower relaxation processes associated with SmC* domain formation in the vicinity of the SmC*–N* phase boundary. The enhanced dielectric strength near the transition arises from increased polarizability of finite sized SmC* domains and their interfaces, while the downward shift of the relaxation frequency reflects the growing dominance of domain-mediated dynamics and increased damping due to strong order-parameter fluctuations. The explanation was further confirmed by the application of a DC bias field. Under a 5.0 V DC bias, the dielectric strength is significantly reduced and exhibits much weaker temperature dependence, while the relaxation frequency shows a conventional increase with temperature. This behavior is attributed to field-induced alignment of the spontaneous polarization, which suppresses domain formation and domain-wall

motion, thereby restoring a dielectric response largely governed by the intrinsic Goldstone mode.

References

1 Clark N A & Lagerwall S T, *Appl Phys Lett*, 36 (1980) 899.
2 Patel J S, *Appl Phys Lett*, 60 (1992) 280.
3 Nonaka T, Li J, Ogawa A, Hornung B, Schmidt W, Wingen R & Dübal H-R, *Liq Cryst*, 26 (1999) 1599.
4 Kim D-W, Yu C-J, Lim Y-W, Na J-H & Lee S-D, *Appl Phys Lett*, 87 (2005) 051917.
5 Manjuladevi V, Panarin Yu P, Song J-K, Vij J K & Sadashiva B K, *Appl Phys Lett*, 93 (2008) 093507.
6 Kobayashi S, Miyama T, Akiyama H, Ikemura A & Kitamura M, *Proc Jpn Acad Ser B Phys Biol Sci*, 98 (2022) 493.
7 Guo Q, Yan K, Chigrinov V, Zhao H & Tribelsky M, *Crystals*, 9 (2019) 470.
8 Chen H-M P & Lin C-W, *Proc SPIE*, 7775 (2010) 77750S.
9 Asao Y, Togano T, Terada M, Moriyama T, Nakamura S & Iba J, *Jpn J Appl Phys*, 38 (1999) 5977.
10 Yadav N, Panarin Y P, Vij J K, Jiang W & Mehl G H, *J Mol Liq*, 378 (2023) 121570.
11 Erkoreka A, Mertelj A, Huang M, Aya S, Sebastián N & Martinez-Perdiguero J, *J Chem Phys*, 159 (2023) 184502.
12 Matko V, Gorecka E, Pociecha D, Matraszek J & Vaupotič N, *Phys Rev Res*, 6 (2024) L042017.
13 Uttam R, Yadav N, Sahai M, Belik A, Jiang W, Mehl G H, Vij J K & Panarin Y P, *J Mater Chem C*, 14 (2026) 6808.
14 Perkowski P & Urbańska M, *Mater*, 17 (2024) 3335.
15 Maeda M, Kihara H, Makino A & Suzuki I, *Jpn J Appl Phys*, 37 (1998) 6465.
16 Debnath A, Mandal P K, Węglowska D & Dąbrowski R, *RSC Adv*, 6 (2016) 84369.
17 Das M K, Barman B, Das B, Hamplova V & Bubnov A, *Crystals*, 9 (2019) 473.
18 Hiller S, Biradar A M, Wrobel S & Haase W, *Phys Rev E*, 53 (1996) 641.
19 Biradar A M, Bawa S S & Chandra S, *Phys Rev A*, 45 (1992) 7282.
20 Chen H-M P & Lin C-W, *Appl Phys Lett*, 95 (2009) 083501.
21 Bhattacharyya S S, Rahman M, Mukherjee A, Chaudhuri B K & Wu S L, *Liq Cryst*, 35 (2008) 751.
22 Bhattacharyya S S, Rahman M, Mukherjee A, Chaudhuri B K & Yoshizawa A, *Appl Phys Lett*, 92 (2008) 122909.
23 Cui Y, Zola R S, Yang Y C & Yang D K, *J Appl Phys*, 111 (2012) 063520.
24 Haase W, Hiller S, Pfeiffer M & Beresnev L A, *Ferroelectrics*, 140 (1993) 37.
25 Cole K S & Cole R H, *J Chem Phys*, 9 (1941) 341.
26 Blinc R & Žekš B, *Soft Modes in Ferroelectrics and Antiferroelectrics*, (North-Holland, Amsterdam) (1974).
27 Lagerwall S T, *Ferroelectric and Antiferroelectric Liquid Crystals*, (Wiley-VCH, Weinheim) (1999).
28 Goodby J W *et al*, *Handbook of Liquid Crystals*, 3 (Wiley-VCH, Weinheim) (2014).
29 Fukuda A, Takanishi Y, Isozaki T, Ishikawa K & Takezoe H, *J Mater Chem*, 4 (1994) 997.
30 de Gennes P G & Prost J, *The Physics of Liquid Crystals*, 2nd ed (Oxford University Press, Oxford) (1993).
31 Bahr C & Heppke G, *Phys Rev A*, 41 (1990) 4335.
32 Thoen J, Marynissen H & Van Dael W, *Phys Rev A*, 26 (1982) 2886.
33 Takanishi Y, Ishikawa K, Takezoe H & Fukuda A, *Phys Rev E*, 51 (1995) 400.